

Removing nonlinearity of a homodyne interferometer by adjusting the gains of its quadrature detector systems

Taeho Keem, Satoshi Gonda, Ichiko Misumi, Qiangxian Huang, and Tomizo Kurosawa

Most homodyne interferometers have a quadrature detector system that includes two polarizing beam splitters that cause nonlinearity of the order of a few nanometers by phase mixing. Detectors should have the same gains to reduce nonlinearity under the assumption that there is no loss in optical components. However, optical components exhibit some loss. We show that nonlinearity can be reduced to an order of 0.01 nm when the detector gains are adjusted by simulation to include the optical characteristics. The compensated nonlinearity is 18 times smaller than that when the four detector gains are set to be equal. © 2004 Optical Society of America

OCIS codes: 000.2170, 120.3180, 120.3930.

1. Introduction

As the demand for integration of silicon chips increases, an accurate method for measuring features smaller than 50 nm will be required by the year 2014,¹ indicating that the required national laboratory metrology precision should be guaranteed within approximately 0.4 nm.² One of the candidate measurement methods is metrological atomic-force microscopy, which is traceable to national length standards by use of a laser interferometer as a tool for displacement measurement. To guarantee the required precision, the measurement uncertainty of the interferometer should be less than 0.1 nm. Because the nonlinearity of an interferometer used for displacement measurement is one of the dominant factors in measurement uncertainty, the current state-of-the-art nonlinearity of the order of 1 nm should be reduced to even less than 0.1 nm. In this paper we discuss the nonlinearity of a homodyne interferometer.

The major cause of nonlinearity of a homodyne interferometer with a quadrature detector system is

phase mixing that is induced by imperfections of optical components such as polarizing beam splitters (PBSs) and wave plates and by misalignment of the axis of the optics with the polarized beam.^{3–10} Because the alignment can be adjusted as precisely as required, the most important source of nonlinearity is imperfection of the optical components. This nonlinearity has been investigated in many studies that aimed to reduce it by changing the interferometer's configuration.^{11–13} However, as Heydemann pointed out,³ the precision and accuracy of interferometers with quadrature detector systems are often limited not by the interferometer itself but by the detector systems. To remove nonlinearity, Heydemann,³ Birch,⁴ and Wu *et al.*⁷ fitted a quadrature signal into a general elliptical equation by the least-squares method and calibrated nonlinear coefficients from the calculated parameters of the general elliptical equation before a real measurement was made. Therefore the output of a homodyne interferometer should be calibrated before real displacement measurements are made. Gonda *et al.*⁹ reported a calibrated nonlinearity of the order of 0.1 nm.

Most homodyne interferometers consist of several PBSs and wave plates. Most PBSs have different optical properties with respect to *p*- and *s*-polarized beams; that is, there is a different transmittance and reflectance for each perpendicularly polarized beam. And there is leakage of an unwanted beam; for example, a little bit of an *s*-polarized beam can pass through the *p*-polarized beam direction, which corresponds to the polarization extinction ratio, i.e., non-zero in a real case, and induces phase mixing. Another factor is optical loss. This optical loss indi-

T. Keem (t-kimu@aist.go.jp), S. Gonda, I. Misumi, Q.-X. Huang, and T. Kurosawa are with the National Metrology Institute of Japan, National Institute of Advanced Industrial Science and Technology, Tsukuba Central 3, 1-1-1 Umezono, Tsukuba, Ibaraki 305-8563, Japan. T. Keem is also with the Billionth Uncertainty Precision Engineering Research Group, Korea Advanced Institute of Science and Technology, Science Town, Daejeon 305-701, Republic of Korea.

Received 1 May 2003; revised manuscript received 2 February 2004; accepted 3 February 2004.

0003-6935/04/122443-06\$15.00/0

© 2004 Optical Society of America

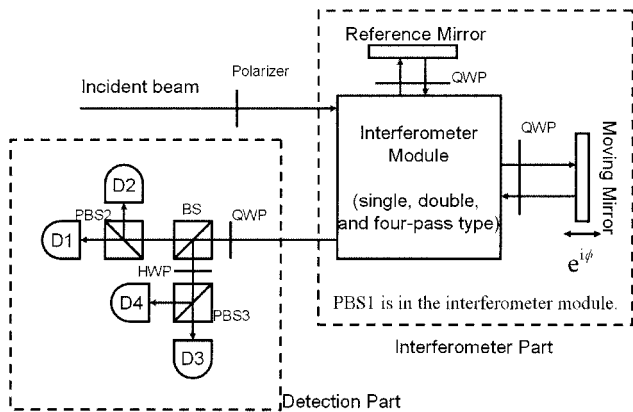


Fig. 1. General homodyne interferometer with a quadrature detector system; it has two parts, an interferometer part and a detector. BS, beam splitter; other abbreviations defined in text.

icates that the sum of the transmittance and the reflectance for each polarized state beam does not equal 1. Moreover, wave plates may exhibit retardation error; for example, a quarter-wave plate retards the phase by $\pi/2$ plus the undesired error, ϵ , in radians. In this study we investigated the effects of optical characteristics of a PBS and a wave plate on the nonlinearity error of the homodyne interferometer with a quadrature detection system by means of Jones matrix calculations.

2. Homodyne Interferometer with a Quadrature Detector System

Figure 1 shows that a homodyne interferometer with a quadrature detector system is divided into two parts: an interferometric part and a detector part. Generally there is one PBS in the interferometric part and there are two PBSs in the detector part. An incident beam passing through a polarizer has two orthogonally polarized beams: p - and s -polarized beams. These two polarized beams as they pass through the interferometer part experience a phase difference ϕ that is dependent on displacement and are combined. Then the combined beam enters into the detector by passing through a quarter-wave plate (QWP). In the detector part the beam is separated into four beams to generate quadrature signals.

Jones matrix calculation is useful for analyzing the phenomena in an interferometer system.⁵ Now we use Jones matrix calculation to consider the optical phenomena of the homodyne interferometer. The electric field of an incident beam passing through a polarizer can be expressed as

$$\mathbf{E} = \begin{bmatrix} \alpha \\ \beta \end{bmatrix}, \quad (1)$$

where α and β are the amplitudes of p - and s -polarized beams, respectively. The optical compo-

nents of interest here are half-wave plates ($\lambda/2$) with axes at 22.5° and quarter-wave plates ($\lambda/4$) with axes at 45° ; they are written as

$$\begin{pmatrix} \lambda \\ 2 \end{pmatrix} = \frac{i}{\sqrt{2}} \begin{bmatrix} -1 & -1 \\ -1 & 1 \end{bmatrix}, \quad \begin{pmatrix} \lambda \\ 4 \end{pmatrix} = \frac{1}{\sqrt{2}} \begin{bmatrix} 1 & -i \\ -i & 1 \end{bmatrix}. \quad (2)$$

First we assume that the wave plates are ideal, that is, that they are free from retardation errors, and that the angles to the polarized beam are exactly aligned. However, PBSs have different transmittances and reflectances to p - and s -polarized beams, such as

$$\mathbf{T}_j = \begin{bmatrix} T_{pj} & 0 \\ 0 & T_{sj} \end{bmatrix}, \quad \mathbf{R}_j = \begin{bmatrix} R_{pj} & 0 \\ 0 & R_{sj} \end{bmatrix}, \quad (3)$$

where \mathbf{T} and \mathbf{R} are the transmittance matrix and the reflectance matrix, respectively, of a , and the subscript j indicates the number of the PBS: PBS1 is in the interferometer part and PBS2 and PBS3 are in the detector part. T_p and T_s mean the transmittance of p - and s -polarized beams, and R_p and R_s are the reflectances of p - and s -polarized beams, respectively. Under ideal conditions, T_p and R_s are equal to 1 and R_p and T_s are equal to zero, but, practically, T_p and R_s are less than 1 and R_p and T_s are not equal to zero. Electric field vector \mathbf{Tr} emerging from the interferometer part can be written as a Jones matrix as follows:

$$\begin{aligned} \mathbf{Tr}_1 &= \left[\mathbf{R}_1 \begin{pmatrix} \lambda \\ 4 \end{pmatrix} \exp(i\phi) \begin{pmatrix} \lambda \\ 4 \end{pmatrix} \mathbf{T}_1 + \mathbf{T}_1 \begin{pmatrix} \lambda \\ 4 \end{pmatrix} \begin{pmatrix} \lambda \\ 4 \end{pmatrix} \mathbf{R}_1 \right] \mathbf{E}, \\ \mathbf{Tr}_2 &= \left[\mathbf{T}_1 \begin{pmatrix} \lambda \\ 4 \end{pmatrix} \exp(i\phi) \begin{pmatrix} \lambda \\ 4 \end{pmatrix} \mathbf{R}_1 \mathbf{R}_1 \begin{pmatrix} \lambda \\ 4 \end{pmatrix} \exp(i\phi) \begin{pmatrix} \lambda \\ 4 \end{pmatrix} \mathbf{T}_1 \right. \\ &\quad \left. + \mathbf{R}_1 \begin{pmatrix} \lambda \\ 4 \end{pmatrix} \begin{pmatrix} \lambda \\ 4 \end{pmatrix} \mathbf{T}_1 \times \mathbf{T}_1 \begin{pmatrix} \lambda \\ 4 \end{pmatrix} \begin{pmatrix} \lambda \\ 4 \end{pmatrix} \mathbf{R}_1 \right] \mathbf{E}, \\ \mathbf{Tr}_4 &= \left[\mathbf{T}_1 \begin{pmatrix} \lambda \\ 4 \end{pmatrix} \exp(i\phi) \begin{pmatrix} \lambda \\ 4 \end{pmatrix} \mathbf{R}_1 \mathbf{R}_1 \begin{pmatrix} \lambda \\ 4 \end{pmatrix} \exp(i\phi) \begin{pmatrix} \lambda \\ 4 \end{pmatrix} \mathbf{T}_1 \right. \\ &\quad \times \mathbf{T}_1 \begin{pmatrix} \lambda \\ 4 \end{pmatrix} \exp(i\phi) \begin{pmatrix} \lambda \\ 4 \end{pmatrix} \mathbf{R}_1 \mathbf{R}_1 \begin{pmatrix} \lambda \\ 4 \end{pmatrix} \exp(i\phi) \begin{pmatrix} \lambda \\ 4 \end{pmatrix} \mathbf{T}_1 \\ &\quad \left. + \mathbf{R}_1 \begin{pmatrix} \lambda \\ 4 \end{pmatrix} \begin{pmatrix} \lambda \\ 4 \end{pmatrix} \mathbf{T}_1 \mathbf{T}_1 \begin{pmatrix} \lambda \\ 4 \end{pmatrix} \begin{pmatrix} \lambda \\ 4 \end{pmatrix} \mathbf{R}_1 \mathbf{R}_1 \begin{pmatrix} \lambda \\ 4 \end{pmatrix} \begin{pmatrix} \lambda \\ 4 \end{pmatrix} \mathbf{T}_1 \right. \\ &\quad \left. \times \mathbf{T}_1 \begin{pmatrix} \lambda \\ 4 \end{pmatrix} \begin{pmatrix} \lambda \\ 4 \end{pmatrix} \mathbf{R}_1 \right] \mathbf{E}, \end{aligned} \quad (4)$$

where vectors \mathbf{Tr}_1 , \mathbf{Tr}_2 , and \mathbf{Tr}_4 indicate the transmitted beam vectors of single-, double- and four-pass-type interferometers, respectively. The electric field vectors after they have passed through the PBS have main electric components \mathbf{E}_i and undesirable components \mathbf{e}_i . Ideally, \mathbf{e}_i should be equal to zero; however these undesirable electric fields \mathbf{e}_i have finite values in practice, so they appear as phase-mixing compo-

nents, where a subscript i indicates the number of detectors:

$$\begin{aligned} \mathbf{D}_1 &= \frac{1}{\sqrt{2}} \mathbf{T}_2 \left(\frac{\lambda}{4} \right) \mathbf{Tr}_i = \begin{pmatrix} E_1 \\ e_1 \end{pmatrix}, \\ \mathbf{D}_2 &= \frac{1}{\sqrt{2}} \mathbf{R}_2 \left(\frac{\lambda}{4} \right) \mathbf{Tr}_i = \begin{pmatrix} e_2 \\ E_2 \end{pmatrix}, \\ \mathbf{D}_3 &= \frac{1}{\sqrt{2}} \mathbf{T}_3 \left(\frac{\lambda}{2} \right) \left(\frac{\lambda}{4} \right) \mathbf{Tr}_i = \begin{pmatrix} E_3 \\ e_3 \end{pmatrix}, \\ \mathbf{D}_4 &= \frac{1}{\sqrt{2}} \mathbf{R}_3 \left(\frac{\lambda}{2} \right) \left(\frac{\lambda}{4} \right) \mathbf{Tr}_i = \begin{pmatrix} e_4 \\ E_4 \end{pmatrix}. \end{aligned} \quad (5)$$

To determine the electric field to be used in the calculation of the intensities to be monitored by detectors we should extract the components, from the vectors including the undesirable components, by means of row vectors whose components are 1 and 0, and 0 and 1, as follows:

$$\begin{aligned} \hat{E}_1 &= (1, 0)\mathbf{D}_1 + (1, 0)\mathbf{D}_2 = E_1 + e_2, \\ \hat{E}_2 &= (0, 1)\mathbf{D}_2 + (0, 1)\mathbf{D}_1 = E_2 + e_1, \\ \hat{E}_3 &= (1, 0)\mathbf{D}_3 + (1, 0)\mathbf{D}_4 = E_3 + e_4, \\ \hat{E}_4 &= (0, 1)\mathbf{D}_4 + (0, 1)\mathbf{D}_3 = E_4 + e_3. \end{aligned} \quad (6)$$

In Eqs. (6), \hat{E}_i means the resultant electric field. Each of these electric fields consists of a main component E_i and an undesirable component e_i of electric field vector \mathbf{D}_i of Eqs. (5). The first and the third electric fields, \hat{E}_1 and \hat{E}_3 , are the sum of the first components of \mathbf{D}_1 , \mathbf{D}_2 and \mathbf{D}_3 , \mathbf{D}_4 , respectively. Likewise, \hat{E}_2 and \hat{E}_4 consist of the second components of \mathbf{D}_1 , \mathbf{D}_2 and \mathbf{D}_3 , \mathbf{D}_4 , respectively. The first terms on the right-hand sides of Eqs. (6) are the desired main electric fields, and the second terms are the undesired terms, that is, they denote cross-talk caused by imperfection of the PBSs on the right-hand side. Now we can obtain the intensity signals through a preamplifier with adjustable gain k_i :

$$I_i = k_i \hat{E}_i \hat{E}_i^*, \quad (7)$$

where i takes values 1–4.

The intensity detected on each detector has an almost 90° phase difference from the each other detector. Thus we can obtain two phase-quadrature signals by subtracting the value of one detector from that of another, and the signals can be expressed as

$$I_x = I_3 - I_4 = D + E \cos(n\phi), \quad (8)$$

$$I_y = I_1 - I_2 = A + B \sin(n\phi + \delta), \quad (9)$$

where n is the number of beam passes, A and D are offsets, B and E are amplitudes, and δ is the differ-

ence from quadrature phase, that is, the phase difference error. To investigate the phase difference we can rewrite Eq. (9) as

$$\begin{aligned} I_y &= A + B \sin(n\phi + \delta) \\ &= A + \gamma \cos(n\phi) + C \sin(n\phi), \end{aligned} \quad (10)$$

where γ appears as a phase-mixing term. From Eqs. (8) and (10) we can derive simple conditions for removing cyclic error, such as that A , γ , and D should be zero and $C = E$. If these conditions are satisfied, we can obtain the nonlinearity's free phase by using the arctangent of

$$\frac{I_y}{I_x} = \frac{I_1 - I_2}{I_3 - I_4} = \frac{\sin(n\phi)}{\cos(n\phi)}. \quad (11)$$

However, parameters A , γ , and D are not zero, and C is not equal to E . Thus, from Eqs. (8) and (10), the desired phase difference is calculated as follows:

$$\phi = \frac{1}{n} \tan^{-1} \left[\frac{E(I_y - A)}{C(I_x - D)} - \frac{\gamma}{C} \right]. \quad (12)$$

The parameters of the elliptical equation fitted by the Heydemann method³ show the relationships among A , γ , C , D , and E , which contribute to the offset from the origin, the difference in major and minor axis lengths, and the rotation of the coordinates of the ellipse. We substituted Eqs. (1)–(7) for the parameters of Eqs. (8) and (10), so we can write each parameter in detail as follows:

$$\begin{aligned} A &= -(\alpha^2 + \beta^2)(T_{p1}{}^{2n}R_{s1}{}^{2n} + R_{p1}{}^{2n}T_{s1}{}^{2n})[k_1(T_{p2} \\ &\quad + R_{p2})^2 - k_2(T_{s2} + R_{s2})^2], \\ \gamma &= -2(\alpha^2 + \beta^2)[k_1(T_{p2} + R_{p2})^2 - k_2(R_{s2} \\ &\quad + T_{s2})^2]T_{p1}{}^nR_{p1}{}^nT_{s1}{}^nR_{s1}{}^n, \\ C &= 2\alpha\beta(T_{p1}{}^{2n}R_{s1}{}^{2n} - R_{p1}{}^{2n}T_{s1}{}^{2n})[k_1(T_{p2} + R_{p2})^2 \\ &\quad + k_2(T_{s2} + R_{s2})^2], \\ D &= k_3(T_{p3} + R_{p3})^2[4\alpha\beta T_{p1}{}^nR_{p1}{}^nT_{s1}{}^nR_{s1}{}^n + (\alpha^2 + \beta^2) \\ &\quad \times (T_{p1}{}^{2n}R_{s1}{}^{2n} + R_{p1}{}^{2n}T_{s1}{}^{2n})] + k_4(T_{s3} \\ &\quad + R_{s3})^2[4\alpha\beta T_{p1}{}^nR_{p1}{}^nT_{s1}{}^nR_{s1}{}^n - (\alpha^2 + \beta^2) \\ &\quad \times (T_{p1}{}^{2n}R_{s1}{}^{2n} + R_{p1}{}^{2n}T_{s1}{}^{2n})], \\ E &= 2\{k_3(T_{p3} + R_{p3})^2[(\alpha^2 + \beta^2)T_{p1}{}^nR_{p1}{}^nT_{s1}{}^nR_{s1}{}^n \\ &\quad + \alpha\beta(T_{p1}{}^{2n}R_{s1}{}^{2n} + R_{p1}{}^{2n}T_{s1}{}^{2n})] - k_4(T_{s3} \\ &\quad + R_{s3})^2[(\alpha^2 + \beta^2)T_{p1}{}^nR_{p1}{}^nT_{s1}{}^nR_{s1}{}^n \\ &\quad - \alpha\beta(T_{p1}{}^{2n}R_{s1}{}^{2n} + R_{p1}{}^{2n}T_{s1}{}^{2n})]\}. \end{aligned} \quad (13)$$

Here, because T_s and R_p have very small values, multiplying T_s by R_p can yield zero. Then, on the basis of the conditions that parameters A , γ , and D

are all zero, and $C = E$, we can obtain the following conditions for eliminating the nonlinearity error:

$$\frac{k_1}{k_2} = \frac{(T_{s2} + R_{s2})^2}{(T_{p2} + R_{p2})^2}, \quad (14)$$

$$\frac{k_3}{k_4} = \frac{(T_{s3} + R_{s3})^2}{(T_{p3} + R_{p3})^2}, \quad (15)$$

$$\frac{k_1(T_{p2} + R_{p2})^2 + k_2(T_{s2} + R_{s2})^2}{k_3(T_{p3} + R_{p3})^2 + k_4(T_{s3} + R_{s3})^2} = 1. \quad (16)$$

If conditions (14) and (15) are satisfied, condition (16) becomes

$$\frac{k_1(T_{p2} + R_{p2})^2}{k_3(T_{p3} + R_{p3})^2} = 1 \quad \text{or} \quad \frac{k_2(T_{s2} + R_{s2})^2}{k_4(T_{s3} + R_{s3})^2} = 1. \quad (17)$$

In addition, if all the optical properties of the PBSs are the same, that is, if $T_{p1} = T_{p2} = T_{p3} = T_p$, $R_{p1} = R_{p2} = R_{p3} = R_p$, $T_{s1} = T_{s2} = T_{s3} = T_s$, and $R_{s1} = R_{s2} = R_{s3} = R_s$, the conditions become simpler:

$$\frac{k_1}{k_2} = \frac{k_3}{k_4} = \frac{(T_s + R_s)^2}{(T_p + R_p)^2}, \quad (18)$$

$$k_1 = k_3, \quad k_2 = k_4.$$

Note that the conditions concern only the optical properties of the PBSs of the detector part, not those of the interferometer part.

In an ideal case there is no loss in PBSs, that is, $T + R = 1$; thus Eq. (14) indicates that all gains of detectors should be the same to eliminate nonlinearity. However, most PBSs exhibit some loss; therefore all gains of the detectors should be adjusted with regard to the transmittance and the reflectance.

3. Simulation

Suppose that the wave plate has no retardation error ϵ , that all optical alignments are perfect, and that there is no noise when intensities are measured. Then the specifications for a PBS are that the transmittances for p - and s -polarized beams are 95% and 0.01%, that is, $T_p = 0.95$ and $T_s = 0.0001$, and the reflectances for p - and s -polarized beams are 5% and 99.8%, that is, $R_p = 0.05$ and $R_s = 0.998$, respectively.¹⁴ These values mean that the polarization extinction ratios of the PBSs indicate that there is undesired optical leakage, which induces phase mixing, and nonlinearity error. We also note from the polarization extinction ratio that the PBS exhibits loss for the s -polarized beam, that is, $T_p + R_p = 1$, but that $T_s + R_s = 0.9981$. Even a high-quality PBS has imperfections, as indicated by values given above. Then the ratio of gain is $k_1/k_2 = k_3/k_4 = 0.9962$, from the extinction ratio obtained by Eq. (18). Thus, let $k_1 = k_3 = 9.96$ and $k_2 = k_4 = 10$. Figure 2 shows the

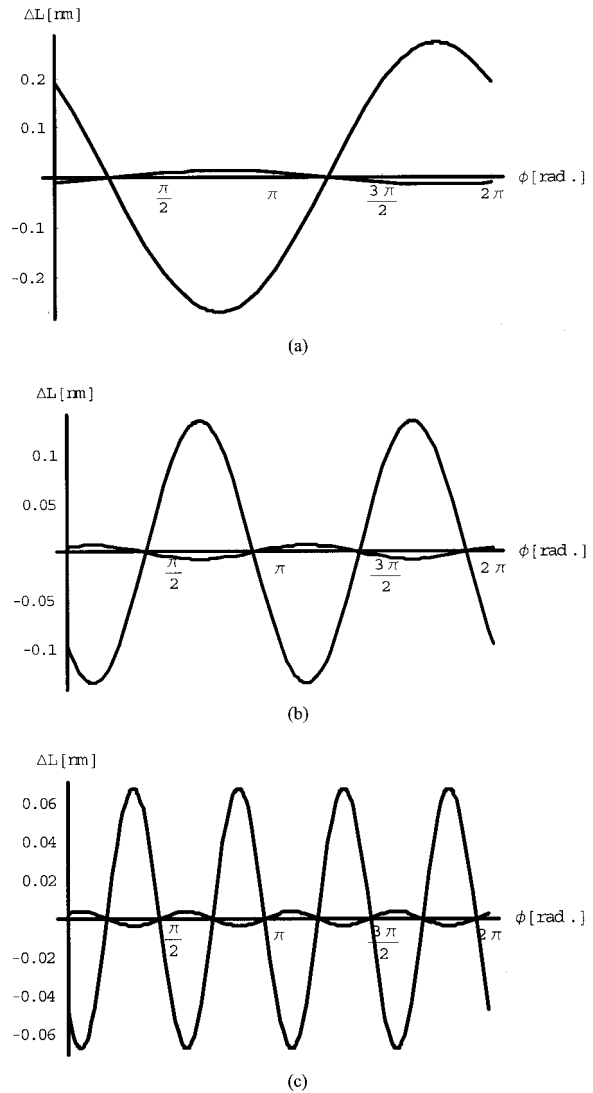


Fig. 2. Remaining error of the homodyne interferometer with a quadrature detector system. After gain adjustment, the remaining error is dramatically reduced by approximately 18×: (a) single-pass interferometer, (b) double-pass interferometer, (c) four-pass interferometer.

remaining error, ΔL , from arctangent calculation of (I_y/I_x) from 0 to 4π :

$$\Delta L = \frac{1}{2\pi} \frac{\lambda}{2} \frac{1}{n} \left[\tan^{-1} \left[\frac{I_y}{I_x} \right] - \tan^{-1} \left[\frac{\sin(n\phi)}{\cos(n\phi)} \right] \right] \quad [\text{nm}]. \quad (19)$$

Figure 2 shows comparisons before and after gain correction: Fig. 2(a) is for a single-pass interferometer, Fig. 2(b) is for a double-pass interferometer, and Fig. 2(c) is for a four-pass interferometer. In Fig. 2 all the highest curves show the nonlinearity error in the absence of gain correction and the all lowest curves show the residual error when the correction is applied. As shown in Fig. 2, the remaining errors are reduced dramatically, by $\sim 18\times$, after gain adjustment. In the four-pass interferometer, after gain

adjustment the remaining error is reduced to ~ 7 pm in the peak-to-peak value. Although the amount of adjustment of the gain is less than 1%, the effect of the adjustment is great. This indicates that the remaining error, on a few-tens-of-picometers level, can be possible only for the single-pass homodyne interferometer with a quadrature detector system.

Next, we considered retardation error ϵ of wave plates. Jones matrix for wave plates W (Ref. 15) with retardation error ϵ can be written as

$$W = \begin{bmatrix} \cos \theta & -\sin \theta \\ \sin \theta & \cos \theta \end{bmatrix} \times \begin{bmatrix} \exp[-i(\Gamma/2 + \epsilon)] & 0 \\ 0 & \exp[i(\Gamma/2 + \epsilon)] \end{bmatrix} \times \begin{bmatrix} \cos \theta & \sin \theta \\ -\sin \theta & \cos \theta \end{bmatrix}. \quad (20)$$

Here, rotation angles θ are 22.5° and 45° to the polarized beam axis, and retardation Γ is π and $\pi/2$ for a half-wave plate and a quarter-wave plate, respectively. Retardation error ϵ is very small, so we can approximate each Jones matrix of the wave plate as

$$\begin{aligned} \left(\frac{\lambda}{4}\right)_{45^\circ} &= \frac{1}{\sqrt{2}} \begin{bmatrix} 1 - \epsilon/2 & -i(1 + \epsilon/2) \\ -i(1 + \epsilon/2) & 1 - \epsilon/2 \end{bmatrix}, \\ \left(\frac{\lambda}{2}\right)_{22.5^\circ} &= \frac{1}{\sqrt{2}} \begin{bmatrix} -i - \epsilon/\sqrt{2} & -i \\ -i & i - \epsilon/\sqrt{2} \end{bmatrix}. \end{aligned} \quad (21)$$

Suppose that the PBSs are perfect, that alignment of all optical components is perfect, and that there is only the error caused by retardation error ϵ of the wave plate. Then we can obtain the intensity as

$$\begin{aligned} I_y &= 1/4 [(\alpha^2 + \beta^2)(-k_1 + k_2) + \epsilon(\alpha^2 - \beta^2)(k_1 + k_2) \\ &\quad + 2\alpha\beta(k_1 + k_2)\sin(n\phi)], \\ I_x &= 1/4 \left[(\alpha^2 + \beta^2)(k_3 - k_4) + \frac{\epsilon}{\sqrt{2}}(\alpha^2 - \beta^2)(k_3 + k_4) \right. \\ &\quad \left. + 2\alpha\beta(k_3 + k_4)\cos(n\phi) \right]. \end{aligned} \quad (22)$$

Note that there is no phase-mixing term because PBSs are assumed to be perfect. In Eqs. (22), if the amplitudes of the incident polarized beams are nearly equal, $\alpha \cong \beta$, multiplying retardation error ϵ by $(\alpha^2 - \beta^2)$ can cancel out ϵ because it is very small. Then the retardation error of wave plates disappears and all gains of the detectors are the same, thus removing the remaining error. Therefore, if there is no loss of the PBSs, the same amplitudes of the incident polarized beams and the same gains of the detectors can remove the nonlinearity of a homodyne interferometer with a quadrature detector system.

We obtained the simulation result of a two-cycle error, i.e., a second-order phase error of two cycles per fringe, only in the case of retardation error. Wu and Su⁶ pointed out that there is only a two-cycle nonlinearity error caused by phase mixing in a homodyne

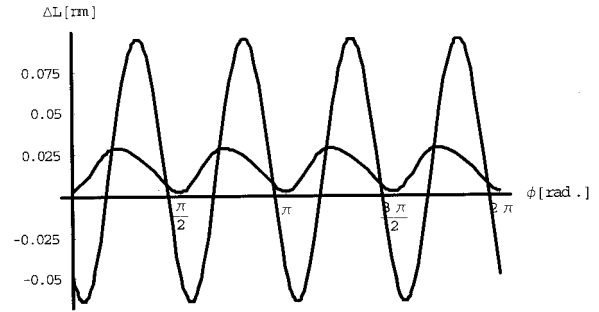


Fig. 3. Remaining error of the four-pass homodyne interferometer; all wave plates have retardation error ϵ in $\lambda/500$. When all the gains of the detectors are equal to 10, the PV value is ± 0.078 nm, but after gain adjustment the PV value is ± 0.013 nm, an $\sim 6\times$ reduction. The reduced signal is biased.

interferometer, but in our investigation the phase-mixing term was so small that the two-cycle error pointed out by Wu *et al.* was not observed and the two-cycle nonlinearity error was observed only when there was no phase mixing caused by PBSs and there was some retardation error of wave plates. Figure 3 shows the remaining error for only the four-pass interferometer with imperfect PBSs and wave plates with a retardation error ϵ of $\lambda/500$.¹⁶ In this case, after gain adjustment, an $\sim 6\times$ reduction effect could be obtained, and a biased remaining error was calculated.

Finally, we introduced a random noise level of 0.5% when intensities were measured. Figure 4 shows a simulation result of ± 0.075 nm in terms of PV value. This result can be available for the fabrication of a more-accurate homodyne interferometer with a quadrature detector system.

We intend to verify these simulation results by making appropriate experiments. At least two experiments will be required: one to measure transmittance and reflectance of PBSs in the detector and the other to verify the result of the measurement. For verifying these results, gain-adjustable detector modules are required. These gain-adjustable detector modules can be achieved easily by use of a gain-controllable preamplifier. But we should be careful with noise. We intend to use a single-pass-type interferometer for easier configuration and faster verification.

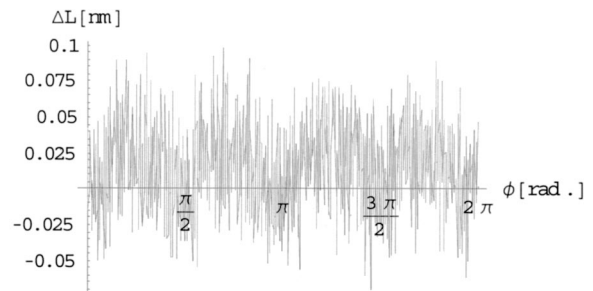


Fig. 4. Simulation result of introducing random noise from measuring the intensities; the PV value is ± 0.075 nm.

4. Conclusions

We have used Jones matrix calculation to investigate the remaining error of a homodyne interferometer with a quadrature detector system. Previously, all the gains of quadrature detector systems were considered to be the same. However, to minimize nonlinearity error from the imperfections of optical components of detector systems, one should adjust the gains of the detectors appropriately, depending on the extinction ratio of the PBSs used. For a high-quality PBS the amount of gain to be adjusted is less than 1%, but adjusting the gain can reduce nonlinearity dramatically. According to our investigation, there was an approximately $18\times$ error-reduction effect. This gain adjustment method for reducing nonlinearity is also applicable for the case in which there is retardation error of wave plates.

We hope to confirm the validity of this method in the near future by experiments that use a single-pass homodyne interferometer for easy verification.

References and Notes

1. T. Ito and S. Okazaki, "Pushing the limits of lithography," *Nature* **406**, 1027–1031 (2000).
2. E. C. Teague, "Generating and measuring displacements up to 0.1 m to an accuracy of 0.1 nm: Is it possible?" in *Technology of Proximal Probe Lithography*, C. R. K. Marrian, ed. (Society of Photo-Optical Instrumentation Engineers, Bellingham, Wash., 1993), pp. 322–363.
3. P. L. M. Heydemann, "Determination and correction of quadrature fringe measurement errors in interferometers," *Appl. Opt.* **20**, 3382–3384 (1981).
4. K. P. Birch, "Optical fringe subdivision with nanometric accuracy," *Precis. Eng.* **12**, 195–198 (1990).
5. V. Greco, G. Molesini, and F. Quercioli, "Accurate polarization interferometer," *Rev. Sci. Instrum.* **66**, 3729–3734 (1995).
6. C.-M. Wu and C.-S. Su, "Nonlinearity in measurement of length by optical interferometry," *Meas. Sci. Technol.* **7**, 62–68 (1996).
7. C.-M. Wu, C.-S. Su, and G.-S. Peng, "Correction of nonlinearity in one-frequency optical interferometry," *Meas. Sci. Technol.* **7**, 520–524 (1996).
8. F. Petru and O. Cip, "Problems regarding linearity of data of a laser interferometer with a single-frequency laser," *Precis. Eng.* **23**, 39–50 (1999).
9. S. Gonda, T. Doi, T. Kurosawa, Y. Tanimura, N. Hisata, T. Yamagishi, H. Fujimoto, and H. Yukawa, "Real-time, interferometrically measuring atomic force microscope for direct calibration of standards," *Rev. Sci. Instrum.* **70**, 3362–3368 (1999).
10. T. B. Eom, J. Y. Kim, and K. Jeong, "The dynamic compensation of nonlinearity in a homodyne laser interferometer," *Meas. Sci. Technol.* **12**, 1734–1738 (2001).
11. M. J. Downs, "A proposed design for an optical interferometer with sub-nanometric resolution," *Nanotechnology* **1**, 27–30 (1990).
12. M. J. Downs and W. R. C. Rowley, "A proposed design for a polarization-insensitive optical interferometer system with subnanometric capacity," *Precis. Eng.* **15**, 281–286 (1993).
13. M. J. Downs, K. P. Birch, M. G. Cox, and J. W. Nunn, "Verification of a polarization-insensitive optical interferometer system with subnanometric capability," *Precis. Eng.* **17**, 84–88 (1995).
14. These specifications are from Spectra-Physics, Inc., <http://www.oriel.com/netcat/VolumeIII/Descrippage/v3t3polbs.htm>.
15. A. Yariv, *Optical Electronics*, 4th ed. (Saunders, Philadelphia, Pa., 1991), Chap. 1.
16. This specification is from ThorLabs Company, http://www.thorlabs.com/ShowProducts.cfm?DID=6&CATID=151&ObjectGroup_ID=152&Queries=1.